Antimicrobial Properties of Graphene Oxide Nanosheets: Why Size Matters

François Perreault, Andreia Fonseca de Faria, Siamak Nejati, and Menachem Elimelech*

Department of Chemical and Environmental Engineering, Yale University, New Haven, Connecticut 06520-8286, United States

ABSTRACT Graphene oxide (GO) is a promising material for the development of antimicrobial surfaces due to its contact-based antimicrobial activity. However, the relationship between GO physicochemical properties and its antimicrobial activity has yet to be elucidated. In this study, we investigated the size-dependency of GO antimicrobial activity using the Gram-negative bacteria *Escherichia coli*. GO suspensions of average sheet area ranging from 0.01 to 0.65 μm^2 were produced and their antimicrobial activity evaluated in cell suspensions or as a model GO surface coating. The antimicrobial activity of GO surface coatings increased 4-fold when GO sheet area decreased from 0.65 to 0.01 μm^2. The higher antimicrobial effect of smaller GO sheets is attributed to oxidative mechanisms associated with the higher defect density of smaller sheets. In contrast, in suspension assays, GO interacted with bacteria in a cell entrapment mechanism; in this case, the antimicrobial effect of GO increased with increasing sheet area, with apparent complete inactivation observed for the 0.65 μm^2 sheets after a 3 h exposure. However, cell inactivation by GO entrapment was reversible and all initially viable cells could be recovered when separated from GO sheets by sonication. These findings provide useful guidelines for future development of graphene-based antimicrobial surface coatings, where smaller sheet sizes can increase the antimicrobial activity of the material. Our study further emphasizes the importance of an accurate assessment of the antimicrobial effect of nanomaterials when used for antimicrobial surface design.

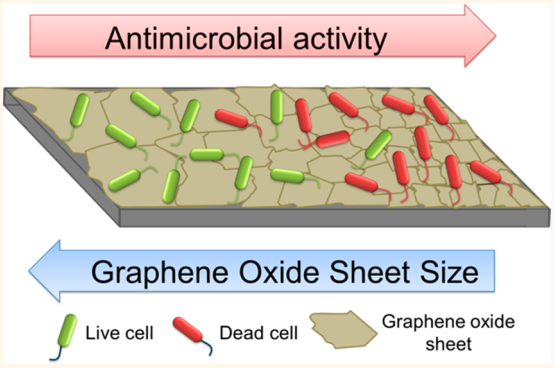

KEYWORDS: graphene oxide · bacterial toxicity · oxidative damage · antimicrobial surfaces · glutathione

Graphene is a two-dimensional carbon nanomaterial consisting of a single layer of sp^2-bonded carbon atoms arranged in a hexagonal crystal structure. Since its first isolation from graphite in 2004,[1] graphene has attracted worldwide interest due to its exceptional electronic, thermal, and mechanical properties.[2] From solar cells to biomedical devices, graphene has opened new possibilities for developing materials with novel or improved properties.[3−5]

A common approach to synthesize graphene materials is based on the use of graphene oxide (GO)—water-dispersible graphene sheets with a high density of oxygen functional groups in the planes and edges of the sheets.[6] GO is produced by the chemical oxidation of graphite to graphite oxide and its subsequent exfoliation by ultrasonication. Due to its low production cost, scalability, and aqueous stability, GO is a very promising material for use as a precursor for chemically reduced graphene or as a building block for graphene-based composite materials.[7]

Several studies have demonstrated the strong antimicrobial properties of GO against a wide variety of microorganisms, including Gram-positive and -negative bacterial pathogens, phytopathogens, and biofilm forming microorganisms.[8−12] The antimicrobial activity of GO is thought to be mediated by physical and chemical interactions when sheets come in direct contact with bacterial cells.[5,13] In this process, the cell membrane appears to be a primary target of the cytotoxicity of GO. Membrane damage in GO-exposed bacteria was identified by morphological changes in the cell structure, leakage of RNA and intracellular electrolytes, uptake of membrane-impermeable dyes, and changes in the transmembrane potential.[8,10,14,15] Membrane damage may be caused by the atomically sharp edges of graphene, which could penetrate the cell membrane and physically disrupt its integrity.[10,14,16] Membrane damage may also be mediated via lipid peroxidation induced by the oxidative nature of GO,[11,12] as was also highlighted for

* Address correspondence to menachem.elimelech@yale.edu.

Received for review April 7, 2015 and accepted June 19, 2015.

Published online June 19, 2015
10.1021/acsnano.5b02067

fullerene[17] and carbon nanotubes (CNTs).[18,19] Oxidative stress was proposed to be a major component of the antimicrobial activity for bacterial cells exposed to GO.[11,12,20]

The antimicrobial properties of GO have triggered a strong interest in the development of GO-based antimicrobial surfaces due to GO's contact-mediated mode of action. This antimicrobial mechanism offers a viable alternative to biocide-releasing surfaces using antibiotics or silver, which deplete from the surface over time.[21] Antimicrobial GO surfaces also avoid the release of toxic biocides, a key consideration in the design of antimicrobial surfaces for environmental applications[22]

Attachment of bacterial cells to GO-coated surfaces was shown to induce a disruption of the cell integrity and loss of cell viability, reducing bacterial development on the surface.[9,10,14,23] GO was successfully used to impart antimicrobial properties to stainless steel,[10] cotton fabric,[24] polymer films,[9,25] and water treatment membranes.[23,26,27] Such antimicrobial surfaces have important applications in the biomedical field for preventing microbial contamination of medical devices, or in environmental systems where biofouling is a major cause of increased operation costs in marine transport, membrane-based water treatment, and heat exchangers.[28−30]

Previous research using CNTs has shown that their cytotoxicity is highly dependent on their physicochemical properties. By changing the size, oxidation level, functionalization, or electronic structure, the cytotoxicity of CNTs may be tuned to increase their antimicrobial potential.[18,19,31−33] However, despite the growing interest in the use of GO for antimicrobial surfaces, there is a limited understanding of the required GO material properties for effective antimicrobial activity. To date, most studies have focused on the antimicrobial properties of GO sheets in suspension assays, where aggregation and cell wrapping mechanisms may occur.[34,35] For example, GO sheet size was found to influence its antimicrobial activity in suspension due to the capacity of larger sheets to completely wrap around the cells and isolate them from their environment.[34] However, in GO-coated surfaces, where sheets are immobilized on the surface, the interactions between GO sheets and bacterial cells may be significantly different than in suspension and changes in the physicochemical properties of GO sheets, such as sheet size, may have a different effect when applied on a surface.

In this study, we investigate how GO sheet size alters the antimicrobial activity of GO-based surface coatings using a model Gram-negative bacteria, *Escherichia coli*. A size dependency in the antimicrobial activity of GO is revealed and explained in terms of changes in the GO material properties and reactivity. Furthermore, the biological interactions of GO in bacterial suspensions and when applied as a surface coating are compared. The differences highlighted in these two distinct exposure conditions demonstrate the importance of selecting antimicrobial nanomaterials based on accurate toxicological data obtained under relevant conditions. Our findings have important implications for the design of novel graphene-based antimicrobial materials.

RESULTS AND DISCUSSION

Characteristics of Graphene Oxide Sheets. GO sheets were obtained by the chemical oxidation of graphite using a modified Hummers' method.[36] This approach generated an oxidized graphite material that can be sonicated to form a well-dispersed aqueous GO suspension which was stable for weeks. AFM imaging revealed that the GO sheets produced by this approach had an average sheet height of 1.4 nm (Figure 1A, B). These results indicate that most sheets were single-layer GO.[37]

The functionalization of graphene by the chemical oxidation treatment is confirmed by Raman spectroscopy and X-ray photoelectron spectroscopy (XPS) (Figure 1C, D). Raman spectroscopy of GO shows the characteristics G (1590 cm^{-1}) and D (1350 cm^{-1}) bands of carbon nanomaterials. The G band is attributed to the sp^2-bonded carbon regions while the D band reflects the amount of disorder introduced to the crystalline structure by the presence of defects.[6,38] The D band, which is absent in pristine graphite, increases in intensity in GO (Figure 1C), indicating the successful oxidation of the graphenic structure. The nature of the oxygen-containing functional groups in GO was identified as C═O, CO, and C═OO bonds by XPS (Figure 1D). Elemental survey by XPS analysis also revealed that

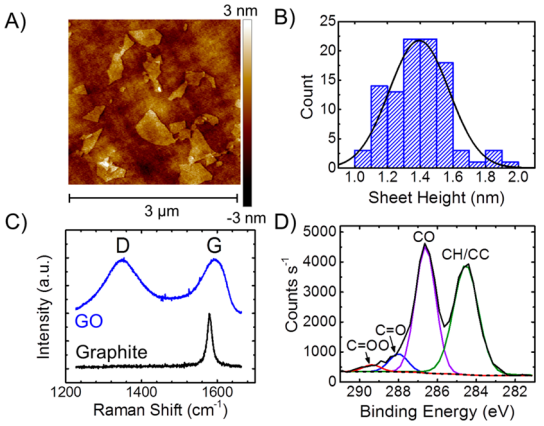

Figure 1. Characteristics of graphene oxide nanosheets. (A) Atomic force microscopy (AFM) imaging of graphene oxide sheets deposited on silicon. (B) Graphene oxide sheet height distribution as determined from AFM imaging. (C) Raman spectra of graphite (black) and graphene oxide (blue). (D) X-ray photoelectron spectroscopy (XPS) of the C 1s region of graphene oxide, indicating the deconvoluted peaks associated with the different carbon functional groups. Experimental data is indicated by a full black line and the baseline by a dotted black line.

GO was free of any metal residues used during the chemical oxidation process (Figure S1, Supporting Information).

To investigate the effect of sheet size on the antimicrobial properties of GO, we generated GO suspensions of different sheet areas using probe sonication (Figure 2). Probe sonicating GO sheets at high power density (6.5 kW L^{-1}) breaks GO sheets into smaller fragments and generates GO sheets of decreasing average area with increasing sonication time.[34,39] The as-synthesized GO sheets, which were dispersed in water by mild bath sonication, have an average sheet area of 0.65 μm^2, with large sheets of up to several micrometers in lateral dimensions (Figure 2B). When the GO suspension is sonicated at high intensity for different periods of time, the average sheet area decreases from 0.65 μm^2 (0 min) to 0.29, 0.10, and 0.01 μm^2 after 1, 10, and 120 min of sonication, respectively (Figure 2A). The complete size distribution of GO sheets at each sonication time is given in Figure S2 of the Supporting Information. This approach provided a wide range of GO sheet dimensions to investigate the effect of sheet size on the antimicrobial activity of GO.

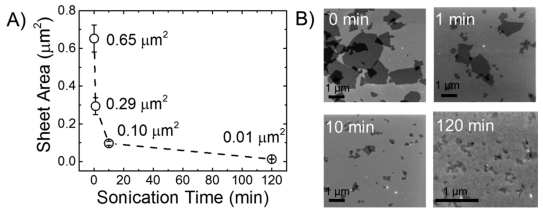

Figure 2. Change in GO sheet area by ultrasonication treatment. (A) Mean GO sheet area for different sonication time. (B) Representative SEM micrographs of the GO sheets deposited on silicon. Images were taken at an acceleration voltage of 2 kV.

Size-Dependent Antimicrobial Activity of Graphene Oxide-Coated Surfaces. The antimicrobial properties of GO of different sheet area were evaluated using model GO-coated surfaces formed by vacuum filtration of a GO suspension over a mixed cellulose filter. After air drying, a stable and homogeneous GO surface is formed (Figure S3). This GO surface is similar to the free-standing antimicrobial GO paper previously developed by Hu et al.[14] Using this model surface, the effect of sheet size on the antimicrobial activity on GO-coated surfaces can be investigated without confounding factors, such as nonuniform surface coverage that could arise from using a GO-functionalized surface.

After 3 h of contact with GO-coated surfaces, *E. coli* cell viability was evaluated using a Live/Dead fluorescent staining, which stains as "dead" those bacteria with compromised membrane integrity.[40] Cell viability was evaluated for planktonic cells, not in contact with GO, and for cells attached to the surface. No change in cell viability was observed for bacterial cells not in contact with the surface, while cell viability decreased for cells attached to all GO surfaces (Figure 3A). These results demonstrate the need for direct contact between bacterial cells and GO for bacterial inactivation, in agreement with the contact-based antimicrobial mechanisms proposed for GO.[10,41] The requirement for cell contact was also highlighted for the toxicity of fullerene[17] and CNTs.[19,31,42] For these materials, intimate contact with

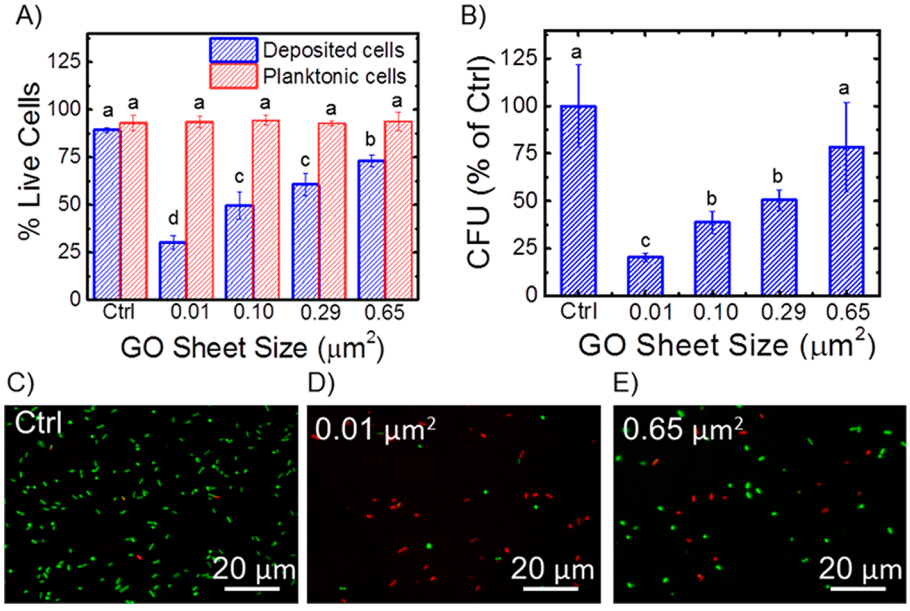

Figure 3. Antimicrobial activity of GO-coated filters for different GO sheet areas. (A) Cell viability of deposited and planktonic *E. coli* cells after 3 h of contact with GO-coated filters, determined by Live/Dead fluorescent staining. (B) Number of viable *E. coli* cells after 3 h of contact with GO-coated filters, determined by CFU agar plate counting. (C–E) Representative epifluorescence picture of live (green) and dead (red) *E. coli* cells on a control surface (mixed-cellulose filter, C) or surfaces coated with GO sheets of 0.01 μm^2 (D) and 0.65 μm^2 (E). Lower case letters in the figure indicate statistical significance, with different letters indicating statistical difference (p-value < 0.05).

the cells allows for direct oxidation of cellular components by the material.[17,19] Physical disruption of the cell membrane may also arise from the interaction between carbon nanomaterials and the cell surface.[42,43] For GO, both these mechanisms have been proposed to explain its antimicrobial activity.[10,12,16,41]

For cells deposited on the surface, a higher number of dead cells are observed when cells are attached to GO-coated surfaces than to a control mixed-cellulose membrane (Figure 3C–E). Cell inactivation by GO is found to be affected by the size of the GO sheets on the surface. For GO sheets of an average area of 0.65, 0.29, 0.10, and 0.01 μm^2, cell viability of deposited cells after 3 h of exposure is 73, 61, 50, and 30%, respectively (Figure 3A). Therefore, the antimicrobial activity of GO sheets, when applied as a surface coating, increases with decreasing sheet dimensions.

The higher antimicrobial activity of small GO sheets contrasts with previous findings where cell inactivation induced by GO in bacterial suspensions increased with increasing sheet size.[34] Since toxicity results from dye-based assays may be affected by interactions of nanomaterials with dye molecules,[44,45] the antimicrobial activity of GO was further confirmed using a second assay. After bacterial exposure, the GO-coated surfaces were mildly washed to remove bacterial cells not attached to the surface. The surfaces were then bath-sonicated to detach the cells, which were immediately spread on agar plates and incubated overnight. Using this dye-independent approach, a similar relationship between GO sheet area and bactericidal activity was found (Figure 3B). Cell inactivation decreased from 79% to 21% when GO sheet area was reduced from 0.65 to 0.01 μm^2, respectively. These consistent results from two independent assays confirm the increasing antimicrobial activity of GO as sheet area is decreased.

Oxidative-Stress Mediated Antimicrobial Activity of Graphene Oxide. Bacterial inactivation by GO, for all sheet areas, was characterized by a disruption of cell integrity. This is demonstrated by the uptake of the membrane impermeable propidium iodide dye in the Live/Dead fluorescent staining (Figure 3D, E), and morphological changes observable by scanning electron microscopy (SEM) (Figure 4). After exposure to GO, cells were fixed in paraformaldehyde-glutaraldehyde, carefully dehydrated, and chromium-coated for microscopy analysis. Figure 4A shows *E. coli* cells with intact cell morphology when deposited on the control mixed-cellulose membrane. On the other hand, bacterial cells deposited on GO-coated surfaces show a flattened or deformed shape, indicative of compromised cell integrity (Figure 4B–D). These results confirm the findings of previous studies where exposure of bacterial cells to GO sheets resulted in alteration of the cell morphology.[8,14,16,23]

In agreement with the fluorescent viability assay, more cells with an altered cell morphology were found

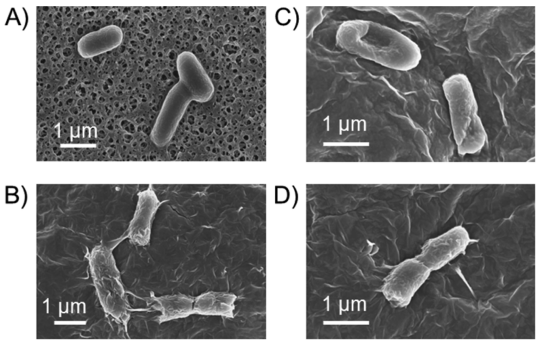

Figure 4. (A) Representative SEM micrographs of *E. coli* cells deposited on a control filter. (B) SEM micrographs of *E. coli* cells deposited on 0.01 μm^2 GO sheets showing compromised cell integrity. (C, D) SEM micrographs of *E. coli* cells deposited on 0.65 μm^2 GO sheets showing compromised (C) and normal (D) cell integrity.

on surfaces coated with small (0.01 μm^2) GO sheets than with large (0.65 μm^2) GO sheets, where cells with normal cell integrity (Figure 4D) were more abundant than cells with compromised cell integrity (Figure 4C). Therefore, although direct contact with GO sheets is required for cell inactivation, additional factors are involved in the extent of bacterial inactivation by GO sheets of different sizes. Additional SEM micrographs of cells on control and GO-coated surfaces can be found in Figure S4 of the Supporting Information.

Previous studies have proposed that physical interactions between GO sheets and bacterial cells may be involved in GO-induced membrane damage. Membrane perturbation and piercing by GO sheets was primarily identified by molecular dynamics (MD) simulations using model phospholipid bilayers.[16,46,47] Interaction between GO sheets and lipid bilayers was found to induce a local perturbation of the lipid bilayer. In these simulations, the highest perturbation was observed for large and unoxidized graphene sheets, while GO sheets, due to their hydrophilicity, mostly adhere on the surface of the membrane without penetrating the lipid bilayer.[47] Other simulations have shown that, in order to penetrate the lipid bilayer, contact must be made through the edges of graphene sheets. The sharp, atomically thin edges of graphene sheets induce a spontaneous piercing of the membrane, which decreases the energy barrier for their penetration into the membrane. Uptake of graphene and GO was identified in mammalian cell lines;[46,48] yet uptake and physically induced membrane damage still remain to be demonstrated in bacterial cells, which differ considerably in their cellular architecture.[49] A recent force spectroscopy investigation of the interactions between GO sheets and *E. coli* cells has shown that the interactions of GO in contact with bacterial cells are mostly repulsive and therefore unfavorable for physically induced membrane damage.[20]

Recent studies have indicated that availability of the basal planes, rather than sheet edges, determines

the antimicrobial properties of GO.[15,50] In Langmuir–Blodgett films, where the sheets are completely flat on the surface and minimal cell contact with the sheet edges occurs, GO was still found to inactivate bacterial cells coming in contact with the surface.[50] These findings suggest that contact with the sheet edges, and thus direct piercing of the membrane by GO sheets, is not required for the antimicrobial activity of GO. Consequently, other mechanisms linked to the physicochemical interactions between GO sheets and bacterial cells may have a more important role in the antimicrobial activity of GO sheets.

Several studies have proposed a primary role of oxidative stress in the antimicrobial activity of GO. Oxidative stress in bacterial cells leads to the oxidation of proteins, lipids, and nucleic acid and can ultimately result in membrane damage and cell death. In bacterial cells exposed to GO, oxidative stress was indicated by the dichlorofluorescein and nitro blue tetrazolium assays, which revealed the intracellular accumulation of free radicals and superoxide anions, respectively.[12,51] Acellular oxidation of lipid molecules, glutathione enzymes, and reduced DPPH (2,2-diphenyl-1-picrylhydrazyl) by GO sheets was also observed, suggesting the intrinsic oxidative potential of GO.[11,41,52,53]

The physicochemical properties of carbon nanomaterials can have a major impact on their intrinsic oxidative activity. For graphene, oxidative stress and glutathione oxidation were shown to differ between GO and chemically reduced GO.[41,53] In CNTs, the nature of the oxygen functional groups or the chirality of the tubes have an important impact on their oxidative capacities.[19,32] The oxidative potential of GO sheets of different sizes was therefore investigated to determine if oxidative pathways are involved in the higher antimicrobial activity of smaller GO sheets. The acellular oxidation of glutathione was used as an indicator of the oxidative potential of the material. Glutathione is a thiol-rich tripeptide serving as one of the major cellular antioxidant enzymes. It is present in millimolar concentrations in Gram-negative bacteria, where it is involved in the intracellular oxidative balance,[54] and is also transported outside the cell to protect against external electrophilic compounds.[55,56] Due to its relevance in oxidative stress, the oxidation of glutathione has been widely used as an indicator of the oxidative potential of carbon nanomaterials.[19,32,41,52,57]

Glutathione was exposed to GO sheets in a bicarbonate buffer for 3 h, after which the unoxidized fraction of glutathione was measured spectrophotometrically using Ellman's reaction.[58] Glutathione oxidation was found to be influenced by the size of GO sheets. As the sheet area is decreased from 0.65 μm^2 to 0.01 μm^2, glutathione oxidation increased from 49 to 71% (Figure 5A). The higher glutathione oxidation by small GO sheets indicates that, as the size of the sheets is decreased, the GO material has a higher capacity to induce oxidative stress. The increased oxidative potential of GO as sheet area is decreased likely contributes to the higher antimicrobial activity of small GO sheets. Likewise, higher glutathione oxidation in CNTs of different chirality[19] or oxygen-containing functional groups[32] was previously found to be a good predictor of their potential antimicrobial activity.

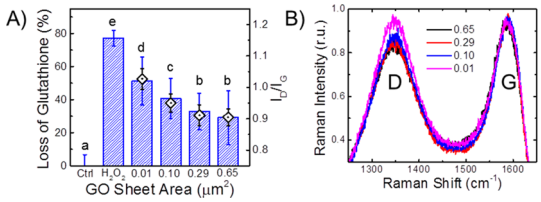

Figure 5. (A) *In vitro* glutathione oxidation by GO sheets of different areas. Glutathione (0.4 mM) was exposed for 3 h to 0 (Ctrl) or 50 μg mL^{-1} GO in 50 mM bicarbonate buffer, pH 8.6. H_2O_2 (1 mM) was used as a positive control for the assay. Black diamond symbols represent the ratio between the D and G bands of GO as measured by Raman spectroscopy. (B) Raman spectra of GO of different sheet areas, showing the characteristics D and G bands. Spectra were normalized to the G band intensity. Lower case letters in (A) indicate statistical significance in glutathione oxidation between treatments, with different letters indicating statistical difference (*p*-value <0.05).

Glutathione oxidation can occur either *via* direct oxidation of biomolecules by GO sheets, as previously indicated for fullerenes,[17] or by an oxygen-mediated, two-step mechanism proposed by Liu et al. for various types of graphenic surfaces.[57] In the oxygen-mediated glutathione oxidation pathway, the first step involves the adsorption of O_2 on defect sites of the graphenic structure, which results in the formation of surface oxides that are reduced by electron transfer from the glutathione enzymes. In the second step, the reduction of these adsorbed oxygen molecules releases reactive oxygen species (H_2O_2 or O_2^-), which are also reduced by the action of glutathione. In the presence of oxygen and cellular antioxidants, GO can therefore lead to oxidative stress either by the direct formation of reactive oxygen species or by the depletion of cellular antioxidants.[57]

According to this oxygen-mediated mechanism, the capacity of GO sheets to oxidize glutathione will be dependent on the density of defects in the carbon structure, as these defects will allow for more oxygen to be adsorbed on the material.[57] Higher defect densities in smaller GO sheets may therefore explain their higher oxidative potential. The increasing density of defects as GO sheet area is decreased was confirmed by Raman spectroscopy. Figure 5B shows the D and G bands of GO sheets of different sizes. By normalizing the spectra to the G band intensity, a gradual increase in the D band intensity is observed as the size of the GO sheets is decreased (Figure 5B). The I_D/I_G ratio, indicating the amount of defects in the GO sheets, increases from 0.90 to 1.03 (Figure 5A, diamond symbols) when GO sheet area is decreased from 0.65 to 0.01 μm^2.

The change in the I_D/I_G ratio correlates with changes in the glutathione oxidation by the GO sheets ($R^2 = 0.96$, Figure S5), indicating that the higher oxidation capacity of GO sheets, as size is decreased, is due to the increasing amount of defects in the GO sheets.

To identify the nature of the defects contributing to the higher oxidation capacity of GO sheets as sheet area decreases, GO chemical structure was determined by XPS (Figure S6). The XPS analysis indicates only small changes in the chemical structure of GO. Decreasing the GO sheet area from 0.65 to 0.01 μm^2 results in a small decrease in the relative abundance of CO (2.7%) and C═O (1.4%) functional groups, with a concomitant increase in C═OO (0.2%) and CC/CH (6.2%). These results are in agreement with recent findings on the photochemical fragmentation of GO sheets by sunlight.[59] Changes in surface functionalities may influence the chemical reactivity of the material, as observed for multiwalled CNTs following thermal annealing.[32] However, for GO, the changes observed as sheet area decreases are small (<4% for all the oxygen functional groups) and none of the different surface functional groups correlated well with the change in glutathione oxidation (Figure S7). Therefore, the change in the oxidation capacity of GO sheets as sheet area decreases does not appear to be associated with a specific surface functional group.

The general decrease in oxygen functional groups in smaller GO sheets indicates that the defect density observed by Raman spectroscopy does not originate from oxygenated defects. Previous studies have indicated that oxygen adsorption on carbon electrodes may not necessarily involve oxygenated defects.[60] In addition, glutathione oxidation by CNTs was decreased by severe oxidation of the tubes, suggesting that oxygen functional groups do not participate in the oxidation reaction.[57] Changes in the I_D/I_G ratio (Figure 5A) can thus be explained by the formation of smaller sp^2 domains with a higher density of edge-type defects and dangling bonds as sheet area decreases.[38,61] A similar increase in the I_D/I_G ratio was observed upon reduction and fragmentation of GO by sunlight.[59] These type of defects will be predominantly associated with sheets' edges, although vacancies in the basal planes can also be expected.[6] Edge-associated defects are known to serve as oxygen adsorption sites on graphenic surfaces.[57,62] These defects could be available to mediate oxidation even on GO-coated surfaces, where edge-mediated physical interactions with the cell membrane may be less favorable,[50] but where oxygen can still diffuse and adsorb to GO sheets. Direct oxidation by GO sheets may also be involved, as defect sites and edges are known to be highly reactive sites compared to graphene planes.[61]

Due to the close association between GO sheets and cell membranes, lipid peroxidation is considered to be the main oxidative pathway leading to oxidative stress in bacterial cells exposed to GO.[11] Lipid peroxidation is a chain reaction that is initiated by the oxidation of lipid molecules by reactive oxygen species, forming lipid peroxide radicals that will propagate the oxidative damage through the membrane.[63] The chain reaction can be terminated by cellular antioxidants that scavenge free radicals. In lipid peroxidation, the most important antioxidant protection is α-tocopherol (vitamin E), a lipid-soluble antioxidant molecule located inside the cell membrane.[63] To confirm the role of oxidative stress in GO-induced bacterial inactivation, we preincubated bacterial cells with 10 mM α-tocopherol to remove the contribution of oxidative stress in the cell response to GO exposure. This approach was previously shown to effectively alleviate the oxidative stress induced by various types of cellular pro-oxidants.[64,65]

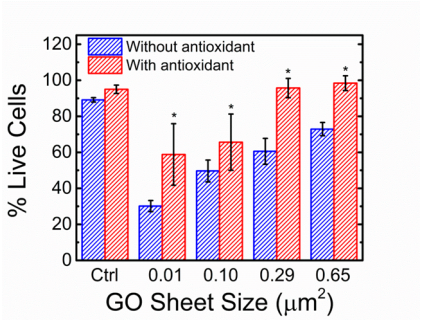

Figure 6. Cell viability of deposited *E. coli* cells after 3 h of contact with GO-coated filters of different GO sheet area, with or without preincubation with 10 mM α-tocopherol (antioxidant). Asterisks indicate statistical difference (*p*-value < 0.05) between treatments with and without antioxidants.

Preincubation of bacterial cells with α-tocopherol reduced the antimicrobial effect of GO exposure for all sheet areas (Figure 6). For the larger GO sheets (0.65 and 0.29 μm^2), the effect of GO was completely nullified and cell viability increased to values similar to the control. These results indicate that oxidative stress was the major contributor to the antimicrobial action of GO. For smaller GO sheets, preincubation with 10 mM α-tocopherol decreased the bacterial inactivation induced by GO, indicating that oxidative stress was also involved in their antimicrobial effect. However, for these smaller, more oxidative GO sheets, cell viability could not be fully recovered by α-tocopherol (Figure 6). This effect can be attributed to the higher oxidative potential of smaller GO sheets, which results in a higher production of reactive species that can overcome the additional protection offered by α-tocopherol preincubation.[64,65] Nonetheless, these results underscore the primary role of oxidative stress in the size-dependency of GO antimicrobial activity. Future studies on the antimicrobial interactions of GO should therefore emphasize the different oxidative interactions of GO-based materials and the resulting oxidative stress at the cellular level.

Apparent Size-Dependent Cell Inactivation in Bacterial Suspension. The size-dependency of the antimicrobial

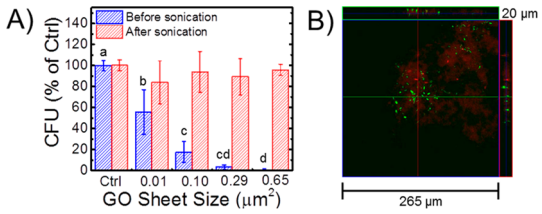

Figure 7. Antimicrobial activity of GO sheets of different sizes in suspension assays. (A) Number of *E. coli* colonies growing on agar plates after 3 h of exposure to 200 μg mL^{-1} GO of different sheet areas, before and after bath sonication to break up GO-bacteria aggregates. (B) Confocal laser scanning microscopy imaging of live (green) and dead (red) cells after 3 h of exposure to 200 μg mL^{-1} of 0.65 μm^2 GO. Side panels show the *z* axis view (height of 20 μm) along the line traced on the image. Lowercase letters in the figure indicate statistical difference (p = 0.05).

activity of GO, when applied on a surface, is found to differ from previous findings based on suspension assays.[34] This discrepancy suggests that the antimicrobial activity of GO involves different interaction mechanisms in suspension assays compared to a GO-based surface coating. To further elucidate the antimicrobial mechanisms of GO, the size-dependency of GO's bactericidal effect was evaluated in cell suspensions. *E. coli* cell suspensions were exposed for 3 h to 200 μg mL^{-1} GO of different sheet sizes and then spread on agar media.

In suspension assays, size was also found to influence the antimicrobial activity of GO (Figure 7A, blue bars). However, when cell inactivation is evaluated using cell suspensions, the size-dependency follows the opposite trend of what was observed for GO surfaces in Figure 3B. After 3 h of exposure, the number of viable CFU decreased from 55 to 0.5% when sheet area increased from 0.01 to 0.65 μm^2, respectively (Figure 7A). These results indicate that larger GO sheets have a more significant effect on bacterial cells in cell suspensions.

The findings described above are in agreement with a previous study by Liu et al.,[34] where larger GO sheets induced a stronger antimicrobial effect, an effect attributed to the capacity of larger sheets to completely cover bacterial cells and prevent their proliferation.[34] Cell entrapment in graphene sheets was also observed by Akhavan et al.,[35] who showed that *E. coli* cells remain viable up to 24 h within the sheets, as they can be reactivated when released from the GO sheets by sonication.[35] In agreement with these previous findings, viable cells in GO-exposed cell suspensions could be completely recovered when separated from the GO sheets. Mild bath sonication was found to restore the number of viable CFU to the level of the control for all GO sheet sizes (Figure 7A, red bars). After sonication, no significant differences between the control samples and the different GO sheet sizes could be found ($p > 0.05$ for all conditions). Our results clearly show that the inhibition of cell proliferation by GO in suspension is reversible, suggesting that the interaction of GO with bacterial cell suspensions does not result in cell inactivation as observed on a GO-coated surface.

To confirm the viability of bacterial cells, cell samples were stained for cell viability at the end of the 3 h exposure and visualized by confocal laser scanning microscopy. Most cells in contact with GO sheets were found to be viable, even under conditions (0.65 μm^2 GO sheets) where complete inactivation appeared to be obtained by CFU count (Figure 7B). In addition, all cells were found within large GO-cell aggregates ranging from 10 to more than 100 μm in size (Figure 7B). These GO-cell aggregates isolated the cells form their media and prevented their proliferation when applied on an agar medium, as suggested in previous studies using suspension assays.[34,35] However, when these aggregates are dispersed by sonication, the viable cells are released into the suspension and therefore cell viability, when evaluated by the CFU method, is recovered (Figure 7A). Our results suggest that antibacterial activity for GO sheets in cell suspensions must be interpreted with caution when correlating toxicity with the physicochemical properties of GO nanomaterials.

An important difference between the antimicrobial interactions of GO with *E. coli* cells in suspensions compared to GO-based surface coatings is the higher viability of cells in contact with GO sheets in the GO-cell aggregates. The high aggregation state may have had an effect on the interaction between cells and GO sheets, which was suggested to be highly orientation-dependent.[15,16,46,50] Membrane damage induced through sheet penetration or phospholipid extraction by GO is mainly mediated by orthogonal contact with GO sheet edges.[16,46] On the other hand, interactions with basal planes were shown to be required, through a still unknown mechanism, for the antimicrobial activity of GO with *E. coli*.[15,50] GO-based surface coatings reduce orthogonal cell contact with sheet edges and enhance interactions with basal planes due to flat sheet stacking. We therefore expect that the interactions between GO-coated surfaces and bacterial cells be different from those observed in suspended aggregates, which possess a looser and undefined structure.

Our results reveal that oxidative stress is a major component of the antimicrobial activity of GO sheets when applied on a surface, an effect that is attributed to the presence of sheet defects which increase the reactivity of the material to biomolecules. However, to clarify the important differences in the antimicrobial effect between GO in suspension and GO surface coatings, the cellular interactions of GO with bacterial systems need to be better understood. Further research should focus on unraveling the oxidative pathways of GO in biological systems and identifying the nature of the defects associated with higher reactivity of GO sheets.

CONCLUSION

GO sheet size was found to have an important influence on the antimicrobial activity of GO, an effect that was dependent on the type of assay used for toxicity evaluation. GO-based surface coatings showed higher antimicrobial activity for smaller GO sheet sizes. The high antimicrobial activity of smaller GO sheets was found to be mediated through oxidative mechanisms due to the higher defect density introduced in GO sheets as size decreases. For cell suspensions, GO sheet area impacted bacterial development by a cell entrapment mechanism. Under these conditions, the antimicrobial activity of GO increased with increasing sheet area. However, cell entrapment was found to be reversible, indicating that the apparent effect of GO does not involve bacterial inactivation and, rather, can be described as bacteriostatic. These findings have important implications for future research on GO-based antimicrobial materials. The size-dependent antimicrobial activity of GO sheets provides useful guidelines for future developments in GO-based antimicrobial surface coatings, where smaller GO sheets may contribute to an improved material performance. Furthermore, the conflicting results between suspension assays and surface coatings emphasize the importance of an accurate assessment of the antimicrobial effect of nanomaterials when used for antimicrobial surface design.

MATERIALS AND METHODS

Materials and Chemicals. Graphite powder (SP-1 grade, 325 mesh) was obtained from Bay Carbon (Bay City, MI). Potassium hydroxide (KOH, >85%), potassium persulfate ($K_2S_2O_8$, 99%), phosphorus pentoxide (P_2O_5, 98%), potassium permanganate ($KMnO_4$, 99%), hydrochloric acid (HCl, 37%), ethanol anhydrous (99.5%), glutaraldehyde (50%), paraformaldehyde (95%), sodium phosphate dibasic heptahydrate ($Na_2HPO_4 \cdot 7H_2O$ >99%), and monobasic potassium phosphate (KH_2PO_4, 99%) were obtained from Sigma-Aldrich (St. Louis, MO). Sulfuric acid (H_2SO_4, 95%) and hydrogen peroxide (H_2O_2, 30%) were obtained from J. T. Baker (Phillipsburg, NJ). 1,1,2-Trichloro-1,2,2-trifluoroethane (Freon, 99%) was purchased from America Refrigerants (Sarasota, FL). Sodium chloride (NaCl, crystals, ACS reagent) was obtained from J. T. Baker (Phillipsburg, NJ). LIVE/DEAD *Bac*Light bacterial viability kit, containing propidium iodide (PI) and SYTO 9, was obtained from Thermo Fisher Scientific (Molecular Probes, Grand Island, NY). Unless specified, all chemicals were dissolved in deionized (DI) water obtained from a Milli-Q ultrapure water purification system (Millipore, Billerica, MA).

Graphene Oxide Synthesis. Single layer graphene oxide (GO) was produced by a modified Hummers' method[66] as previously described.[36] SP-1 graphite (1.0 g) was dispersed in concentrated sulfuric acid (5 mL) and preoxidized using $K_2S_2O_8$ (1.0 g) and P_2O_5 (1.0 g). The mixture was kept at 80 °C for 4.5 h, poured into 160 mL of DI water, and allowed to rest overnight. The graphite powder was collected by vacuum filtration on a 0.45 μm PTFE membrane (Millipore), washed extensively with DI water, and left to dry overnight at room temperature. In the second step, the preoxidized graphite was placed in concentrated sulfuric acid (40 mL), and $KMnO_4$ (5.0 g) was slowly added to the graphite suspension. Care was taken not to let the temperature increase above 10 °C by using an ice bath. After the $KMnO_4$ addition, the mixture was slowly heated to 35 °C and left to react for 2.5 h. DI water (77.0 mL) was then slowly added into the suspension, not allowing the temperature to exceed 50 °C. After water addition, the mixture was left to react for an additional 2 h at room temperature. The solution was then poured into 240 mL of DI water, and 4.2 mL of H_2O_2 (30%) was added, which turned the color of the reaction to a bright yellow. The solution was kept at room temperature for 2 days and the precipitate was recovered by centrifugation (12 000*g*, 30 min) and washed with HCl (10% v/v) and DI water to remove chemical residues. The resulting material was resuspended in DI water and dialyzed with Spectra/Por 3 dialysis membranes (molecular weight cutoff 3500 Da) for 3 days for additional purification. The final dark brown graphite oxide suspension was lyophilized and stored at room temperature until use.

Different GO sheet area distributions were obtained by probe sonication of the initial GO material, as previously described.[34] GO suspensions (2 mg mL^{-1} in DI water) were first bath-sonicated (26 W L^{-1}, FS60 Ultrasonic Cleaner) to obtain a clear stable suspension. Then, GO suspensions were probe-sonicated for 0, 1, 10, and 120 min at high-intensity (6.5 kW L^{-1}, Misonix 3000, Misonix Inc., Farmingdale, NY) to break GO sheets. An ice bath was used to avoid increase in temperature during the sonication process.

Graphene Oxide Characterization. Raman spectra of graphite and GO powders were acquired using a Horiba Jobin Yvon HR-800 Raman spectrometer equipped with a 532 nm laser excitation, 1800 grooves mm^{-1} grating, 300 μm spectrograph entrance confocal hole and 200 μm slit, and a ×100 objective. XPS measurements were performed on a PHI 5000 VersaProbe Instrument (Physical Electronics, Chanhassen, MN), operating with a monochromatic Al Kα X-ray source ($h\nu$ = 1486 eV). High resolution XPS spectrum of C 1s was acquired with a 100 W beam power at 23.5 eV pass energy and 200 ms dwell time for the detector, with the resolution set at 0.2 eV. The spectra were averaged over 20 scans. Atomic force microscopy (AFM) height images were taken in tapping mode with a Bruker Multimode (Digital Instruments, Plainview, NY) AFM equipped with a Tap300Al-G cantilever (BudgetSensors, resonance frequency of 300 kHz). Scanning electron microscopy (SEM) images were taken with a Hitachi SU-70 scanning electron microscope. For both AFM and SEM, 3 μL of a diluted GO (50 μg mL^{-1}) was drop-cast on a 1 cm × 1 cm silicon wafer previously cleaned by a 20 min UV-ozone treatment (UV/Ozone ProCleaner, BioForce Nanosciences, Ames, IA).

Antimicrobial Activity of Graphene Oxide-Coated Surfaces. *Escherichia coli* K12 (Coli Genetic Stock Center #7740) cultures were grown overnight in Luria–Bertani broth at 37 °C. The cultures were then diluted in fresh medium and grown until log phase (~2 h), which was verified by measuring the optical density at 600 nm. The bacterial cells were washed three times with sterile 0.9% NaCl solution before being diluted to 10^7 colony-forming units (CFU) mL^{-1} in sterile saline solution.

For GO exposure, a homogeneous GO surface coating was obtained by filtering a 2 mL GO suspension (200 μg mL^{-1}) on a membrane (0.025 μm mixed cellulose ester, Millipore, Billerica, MA) and air-dried. Then, 2 mL of diluted bacterial suspension were slowly added on top of the GO surface. Bacterial cells were kept in contact with the GO-coated surface for 3 h. After the 3 h incubation, the bacteria suspension was removed and the GO-coated filters were washed with sterile 0.9% NaCl suspension to remove unattached cells. The filters were placed in a 50 mL Falcon tube containing 10 mL of 0.9% saline solution and bath-sonicated (26 W L-1, FS60 Ultrasonic Cleaner) for 10 min to detach bacteria from the surface. Bacteria were then immediately spread on LB agar plates and incubated overnight at 37 °C for CFU enumeration.

Cell viability was determined by using the LIVE/DEAD fluorescent staining assay. Briefly, cells were exposed to GO in the same way as for CFU enumeration. After washing the GO-coated surface, cells deposited on the GO surface were stained

with 3.34 μM SYTO 9 and 20 μM propidium iodide in 0.9% saline solution (Thermo Fisher Scientific, Molecular Probes, Grand Island, NY) for 30 min. The staining solution was removed before mounting the GO with deposited cells on a microscopic slide for epifluorescence microscopy. Ten pictures per replicate were taken with an Axiovert 200 M epifluorescence microscope (Carl Zeiss Inc., Thornwood, NY). Live (green) and dead (red) cells were counted with the ImageJ Cell Counter Plugin (National Institutes of Health, Bethesda, MD).

Cell morphology of bacteria deposited on GO-coated filters was visualized by SEM as previously described.[23] After exposing the cells to GO, the control and GO-coated filters were washed with 0.9% sterile saline solution and fixed with Karnovsky's fixative (2% paraformaldehyde, 2.5% glutaraldehyde in 0.2 M Sorenson's buffer, pH 7.2) for 3 h. Samples were then dehydrated by a sequential immersion (10 min) in water/ethanol (50, 70, 80, 90, 100%) and ethanol/freon (50, 75, 100%), and left to dry overnight in a desiccator at room temperature. Samples were then sputter-coated with chromium and imaged by SEM.

Antimicrobial Activity of Graphene Oxide in Suspension. *E. coli* cultures were grown as described in the previous section. The bacterial cells were washed three times with sterile 0.9% NaCl solution before being diluted to 10^6 colony forming units (CFU) mL^{-1} in sterile saline solution. GO (2 mg mL^{-1} stock) was added to the medium for a final concentration of 200 μg mL^{-1}. Cells were exposed to suspended GO for 3h at room temperature under constant agitation. At the end of the exposure period, bacterial suspensions were plated on LB agar media and incubated overnight at 37 °C for CFU enumeration. To evaluate the viability of cells present in GO aggregates, the bacterial suspensions at the end of the exposure period were bath-sonicated for 10 min to break aggregates, as previously described,[35] and immediately plated on agar media.

Cell viability in GO-bacteria aggregates was determined by LIVE/DEAD fluorescent staining. After the 3 h exposure period, cells were stained by adding 3.34 μM SYTO 9 and 20 μM propidium iodide to the suspension (LIVE/DEAD *Bac*Light viability assay, Invitrogen). The samples were incubated for 30 min in the dark before pipetting 20 μL to a microscope slide. The microscope slide was covered with a coverslip and sealed for confocal laser scanning microscopy measurement. Images were taken with a Zeiss LSM 510 equipped with a Plan-Apochromat 20×/0.8 numerical aperture objective (Carl Zeiss Inc., Thornwood, NY).

Glutathione Oxidation by Graphene Oxide. Glutathione (GSH) oxidation mediated by GO was measured in acellular conditions using a procedure modified from that described in our previous publications.[19,32] Reduced glutathione (0.4 mM) was exposed to GO nanosheets (50 μg mL^{-1}) in a total volume of 10 mL of 50 mM bicarbonate buffer (pH 8.6) in a 25 mL glass scintillation vial. Samples were exposed at room temperature for 3 h in the dark, under constant agitation. The amount of nonoxidized GSH was quantified spectrophotometrically using Ellman's reagent (5,5′-dithiobis(2-nitrobenzoic acid), DTNB), which reacts with thiol groups of GSH to yield 3-thio-6-nitrobenzoate (TNB) in a 1:1 ratio.[67] The reaction medium was filtered with a 0.45 μm poly(ether sulfone) filter unit (Whatman) to remove GO sheets. Then, 900 μL of the filtered reaction mixture were added to 1.57 mL Tris-HCl buffer (pH 8.3) to which 30 μL of 100 mM DTNB was added. The amount of thiol remaining in the reaction medium was quantified by measuring TNB absorbance at 412 nm, using an extinction coefficient of 14 150 M^{-1} cm^{-1}.[58]

Conflict of Interest: The authors declare no competing financial interest.

Acknowledgment. F.P. acknowledges the financial support from the Natural Sciences and Engineering Research Council of Canada postdoctoral fellowship. A.F.F acknowledges the financial support of the Science without Borders program, through the Brazilian Council of Science and Technology (CNPq Grant 246407/2012-3), and the Lemann Institute for Brazilian Studies. Facilities used were supported by the Yale Institute of Nanoscale and Quantum Engineering (YINQE) and NSF MRSEC DMR 1119826. We also thank Prof. Kanani Lee for granting access to the Raman spectrometer and Dr. George Amulele for his technical assistance.

Supporting Information Available: XPS elemental analysis of GO (Figure S1); detailed GO sheet area distributions (Figure S2); SEM micrograph of a pure GO-coated surface, showing homogeneous coverage of the surface (Figure S3); SEM micrographs of *E. coli* cells on GO-coated surfaces of different sheet areas (Figure S4); relationship between glutathione oxidation and the defect density (I_D/I_G ratio) in GO sheets (Figure S5); XPS spectra of GO sheets of different average surface area (Figure S6); and relationship between glutathione oxidation and relative abundance of different functional groups on GO (Figure S7). The Supporting Information is available free of charge on the ACS Publications website at DOI: 10.1021/acsnano.5b02067.

REFERENCES AND NOTES

1. Novoselov, K. S.; Geim, A. K.; Morozov, S. V.; Jiang, D.; Zhang, Y.; Dubonos, S. V.; Grigorieva, I. V.; Firsov, A. A. Electric Field Effect in Atomically Thin Carbon Films. *Science* **2004**, *306*, 666–669.
2. Geim, A. K.; Novoselov, K. S. The Rise of Graphene. *Nat. Mater.* **2007**, *6*, 183–191.
3. Sun, Y.; Wu, Q.; Shi, G. Graphene Based New Energy Materials. *Energy Environ. Sci.* **2011**, *4*, 1113–1132.
4. Bitounis, D.; Ali-Boucetta, H.; Hong, B. H.; Min, D.-H.; Kostarelos, K. Prospects and Challenges of Graphene in Biomedical Applications. *Adv. Mater.* **2013**, *25*, 2258–2268.
5. Perreault, F.; de Faria, A. F.; Elimelech, M. Environmental Applications of Graphene-Based Nanomaterials. *Chem. Soc. Rev.* **2015**, DOI: 10.1039/C5CS00021A.
6. Dreyer, D. R.; Park, S.; Bielawski, C. W.; Ruoff, R. S. The Chemistry of Graphene Oxide. *Chem. Soc. Rev.* **2010**, *39*, 228–240.
7. Compton, O. C.; Nguyen, S. T. Graphene Oxide, Highly Reduced Graphene Oxide, and Graphene: Versatile Building Blocks for Carbon-Based Materials. *Small* **2010**, *6*, 711–723.
8. Chen, J.; Peng, H.; Wang, X.; Shao, F.; Yuan, Z.; Han, H. Graphene Oxide Exhibits Broad-Spectrum Antimicrobial Activity against Bacterial Phytopathogens and Fungal Conidia by Intertwining and Membrane Perturbation. *Nanoscale* **2014**, *6*, 1879–1889.
9. Mejías Carpio, I. E.; Santos, C. M.; Wei, X.; Rodrigues, D. F. Toxicity of a Polymer-Graphene Oxide Composite against Bacterial Planktonic Cells, Biofilms, and Mammalian Cells. *Nanoscale* **2012**, *4*, 4746–4756.
10. Akhavan, O.; Ghaderi, E. Toxicity of Graphene and Graphene Oxide Nanowalls against Bacteria. *ACS Nano* **2010**, *4*, 5731–5736.
11. Krishnamoorthy, K.; Veerapandian, M.; Zhang, L.; Yun, K.; Kim, S. J. Antibacterial Efficiency of Graphene Nanosheets against Pathogenic Bacteria via Lipid Peroxidation. *J. Phys. Chem. C* **2012**, 17280–17287.
12. Gurunathan, S.; Han, J. W.; Dayem, A. A.; Eppakayala, V.; Kim, J.-H. Oxidative Stress-Mediated Antibacterial Activity of Graphene Oxide and Reduced Graphene Oxide in *Pseudomonas Aeruginosa*. *Int. J. Nanomed.* **2012**, *7*, 5901–5914.
13. Sanchez, V. C.; Jachak, A.; Hurt, R. H.; Kane, A. B. Biological Interactions of Graphene-Family Nanomaterials: An Interdisciplinary Review. *Chem. Res. Toxicol.* **2012**, *25*, 15–34.
14. Hu, W.; Peng, C.; Luo, W.; Lv, M.; Li, X.; Li, D.; Huang, Q.; Fan, C. Graphene-Based Antibacterial Paper. *ACS Nano* **2010**, *4*, 4317–4323.
15. Hui, L.; Piao, J.-G.; Auletta, J.; Hu, K.; Zhu, Y.; Meyer, T.; Liu, H.; Yang, L. Availability of the Basal Planes of Graphene Oxide Determines Whether It Is Antibacterial. *ACS Appl. Mater. Interfaces* **2014**, *6*, 13183–13190.
16. Tu, Y.; Lv, M.; Xiu, P.; Huynh, T.; Zhang, M.; Castelli, M.; Liu, Z.; Huang, Q.; Fan, C.; Fang, H.; et al. Destructive Extraction of Phospholipids from *Escherichia Coli* Membranes by Graphene Nanosheets. *Nat. Nanotechnol.* **2013**, *8*, 594–601.

17. Lyon, D. Y.; Alvarez, P. J. J. Fullerene Water Suspension (nC60) Exerts Antibacterial Effects via ROS-Independent Protein Oxidation. *Environ. Sci. Technol.* **2008**, *42*, 8127–8132.
18. Kang, S.; Herzberg, M.; Rodrigues, D. F.; Elimelech, M. Antibacterial Effects of Carbon Nanotubes: Size Does Matter! *Langmuir* **2008**, *24*, 6409–6413.
19. Vecitis, C. D.; Zodrow, K. R.; Kang, S.; Elimelech, M. Electronic-Structure-Dependent Bacterial Cytotoxicity of Single-Walled Carbon Nanotubes. *ACS Nano* **2010**, *4*, 5471–5479.
20. Castrillón, S. R.-V.; Perreault, F.; de Faria, A. F.; Elimelech, M. Interaction of Graphene Oxide with Bacterial Cell Membranes: Insights from Force Spectroscopy. *Environ. Sci. Technol. Lett.* **2015**, *2*, 112–117.
21. Liu, J.; Hurt, R. H. Ion Release Kinetics and Particle Persistence in Aqueous Nano-Silver Colloids. *Environ. Sci. Technol.* **2010**, *44*, 2169–2175.
22. Banerjee, I.; Pangule, R. C.; Kane, R. S. Antifouling Coatings: Recent Developments in the Design of Surfaces That Prevent Fouling by Proteins, Bacteria, and Marine Organisms. *Adv. Mater.* **2011**, *23*, 690–718.
23. Perreault, F.; Tousley, M. E.; Elimelech, M. Thin-Film Composite Polyamide Membranes Functionalized with Biocidal Graphene Oxide Nanosheets. *Environ. Sci. Technol. Lett.* **2014**, 71–76.
24. Karimi, L.; Yazdanshenas, M. E.; Khajavi, R.; Rashidi, A.; Mirjalili, M. Using graphene/TiO2 Nanocomposite as a New Route for Preparation of Electroconductive, Self-Cleaning, Antibacterial and Antifungal Cotton Fabric without Toxicity. *Cellulose* **2014**, *21*, 3813–3827.
25. Santos, C. M.; Tria, M. C. R.; Vergara, R. A. M. V; Ahmed, F.; Advincula, R. C.; Rodrigues, D. F. Antimicrobial Graphene Polymer (PVK-GO) Nanocomposite Films. *Chem. Commun.* **2011**, *47*, 8892–8894.
26. Musico, Y. L. F.; Santos, C. M.; Dalida, M. L. P.; Rodrigues, D. F. Surface Modification of Membrane Filters Using Graphene and Graphene Oxide-Based Nanomaterials for Bacterial Inactivation and Removal. *ACS Sustainabld Chem. Eng.* **2014**, *2*, 1559–1565.
27. Lee, J. J.; Chae, H.-R.; Won, Y. J.; Lee, K.; Lee, C.-H.; Lee, H. H.; Kim, I.-C.; Lee, J. J. Graphene Oxide Nanoplatelets Composite Membrane with Hydrophilic and Antifouling Properties for Wastewater Treatment. *J. Membr. Sci.* **2013**, *448*, 223–230.
28. Melo, L. F.; Bott, T. R. Biofouling in Water Systems. *Exp. Therm. Fluid Sci.* **1997**, *14*, 375–381.
29. Elimelech, M.; Phillip, W. A. The Future of Seawater Desalination: Energy, Technology, and the Environment. *Science* **2011**, *333*, 712–717.
30. Schultz, M. P.; Bendick, J. A; Holm, E. R.; Hertel, W. M. Economic Impact of Biofouling on a Naval Surface Ship. *Biofouling* **2011**, *27*, 87–98.
31. Kang, S.; Mauter, M. S.; Elimelech, M. Physicochemical Determinants of Multiwalled Carbon Nanotube Bacterial Cytotoxicity. *Environ. Sci. Technol.* **2008**, *42*, 7528–7534.
32. Pasquini, L. M.; Sekol, R. C.; Taylor, A. D.; Pfefferle, L. D.; Zimmerman, J. B. Realizing Comparable Oxidative and Cytotoxic Potential of Single- and Multiwalled Carbon Nanotubes through Annealing. *Environ. Sci. Technol.* **2013**, *47*, 8775–8783.
33. Pasquini, L. M.; Hashmi, S. M.; Sommer, T. J.; Elimelech, M.; Zimmerman, J. B. Impact of Surface Functionalization on Bacterial Cytotoxicity of Single-Walled Carbon Nanotubes. *Environ. Sci. Technol.* **2012**, *46*, 6297–6305.
34. Liu, S.; Hu, M.; Zeng, T. H.; Wu, R.; Jiang, R.; Wei, J.; Wang, L.; Kong, J.; Chen, Y. Lateral Dimension-Dependent Antibacterial Activity of Graphene Oxide Sheets. *Langmuir* **2012**, *28*, 12364–12372.
35. Akhavan, O.; Ghaderi, E.; Esfandiar, A. Wrapping Bacteria by Graphene Nanosheets for Isolation from Environment, Reactivation by Sonication, and Inactivation by near-Infrared Irradiation. *J. Phys. Chem. B* **2011**, *115*, 6279–6288.
36. Tung, V. C.; Allen, M. J.; Yang, Y.; Kaner, R. B. High-Throughput Solution Processing of Large-Scale Graphene. *Nat. Nanotechnol.* **2009**, *4*, 25–29.
37. Mcallister, M. J.; Li, J.; Adamson, D. H.; Schniepp, H. C.; Abdala, A. A; Liu, J.; Herrera-alonso, M.; Milius, D. L.; Car, R.; Prud'homme, R. K.; et al. Single Sheet Functionalized Graphene by Oxidation and Thermal Expansion of Graphite. *Chem. Mater.* **2007**, *19*, 4396–4404.
38. Tuinstra, F.; Koenig, L. Raman Spectrum of Graphite. *J. Chem. Phys.* **1970**, *53*, 1126–1130.
39. Akhavan, O.; Ghaderi, E.; Akhavan, A. Size-Dependent Genotoxicity of Graphene Nanoplatelets in Human Stem Cells. *Biomaterials* **2012**, *33*, 8017–8025.
40. Lloyd, D.; Hayes, A. J. Vigour, Vitality and Viability of Microorganisms. *FEMS Microbiol. Lett.* **1995**, *133*, 1–7.
41. Liu, S.; Zeng, T. H.; Hofmann, M.; Burcombe, E.; Wei, J.; Jiang, R.; Kong, J.; Chen, Y. Antibacterial Activity of Graphite, Graphite Oxide, Graphene Oxide, and Reduced Graphene Oxide: Membrane and Oxidative Stress. *ACS Nano* **2011**, *5*, 6971–6980.
42. Kang, S.; Pinault, M.; Pfefferle, L. D.; Elimelech, M. Single-Walled Carbon Nanotubes Exhibit Strong Antimicrobial Activity. *Langmuir* **2007**, *23*, 8670–8673.
43. Liu, S.; Ng, A. K.; Xu, R.; Wei, J.; Tan, C. M.; Yang, Y.; Chen, Y. Antibacterial Action of Dispersed Single-Walled Carbon Nanotubes on *Escherichia Coli* and *Bacillus Subtilis* Investigated by Atomic Force Microscopy. *Nanoscale* **2010**, *2*, 2744–2750.
44. Hurt, R. H.; Monthioux, M.; Kane, A. Toxicology of Carbon Nanomaterials: Status, Trends, and Perspectives on the Special Issue. *Carbon* **2006**, *44*, 1028–1033.
45. Casey, A.; Herzog, E.; Davoren, M.; Lyng, F. M.; Byrne, H. J.; Chambers, G. Spectroscopic Analysis Confirms the Interactions between Single Walled Carbon Nanotubes and Various Dyes Commonly Used to Assess Cytotoxicity. *Carbon* **2007**, *45*, 1425–1432.
46. Li, Y.; Yuan, H.; von dem Bussche, A.; Creighton, M.; Hurt, R. H.; Kane, A. B.; Gao, H. Graphene Microsheets Enter Cells through Spontaneous Membrane Penetration at Edge Asperities and Corner Sites. *Proc. Natl. Acad. Sci. U. S. A.* **2013**, *110*, 12295–12300.
47. Mao, J.; Guo, R.; Yan, L.-T. Simulation and Analysis of Cellular Internalization Pathways and Membrane Perturbation for Graphene Nanosheets. *Biomaterials* **2014**, *35*, 6069–6077.
48. Zhang, X.; Hu, W.; Li, J.; Tao, L.; Wei, Y. A Comparative Study of Cellular Uptake and Cytotoxicity of Multi-Walled Carbon Nanotubes, Graphene Oxide, and Nanodiamond. *Toxicol. Res.* **2012**, *1*, 62.
49. Chen, K. L.; Bothun, G. D. Nanoparticles Meet Cell Membranes: Probing Nonspecific Interactions Using Model Membranes. *Environ. Sci. Technol.* **2014**, *48*, 873–880.
50. Mangadlao, J. D.; Santos, C. M.; Felipe, M. J. L.; Leon, A. C. C.; De Rodrigues, D. F. On the Antibacterial Mechanism of Graphene Oxide (GO) Langmuir – Blodgett Films †. *Chem. Commun.* **2015**, *1*, 1–4.
51. Chen, J.; Wang, X.; Han, H. A New Function of Graphene Oxide Emerges: Inactivating Phytopathogenic Bacterium *Xanthomonas Oryzae* Pv. *Oryzae*. *J. Nanoparticle Res.* **2013**, *15*, 1658.
52. Ahmed, F.; Rodrigues, D. F. Investigation of Acute Effects of Graphene Oxide on Wastewater Microbial Community: A Case Study. *J. Hazard. Mater.* **2013**, *256–257*, 33–39.
53. Kurantowicz, N.; Sawosz, E.; Jaworski, S.; Kutwin, M.; Strojny, B.; Wierzbicki, M.; Szeliga, J.; Hotowy, A.; Lipi, L.; Jagie, J.; et al. Interaction of Graphene Family Materials with *Listeria Monocytogenes* and *Salmonella Enterica*. *Nanoscale Res. Lett.* **2015**, 10–23.
54. Fahey, R. C.; Brown, W. C.; Adams, W. B.; Worsham, M. B. Occurrence of Glutathione in Bacteria. *J. Bacteriol.* **1978**, *133*, 1126–1129.
55. Owens, R. A; Hartman, P. E. Glutathione: A Protective Agent in *Salmonella Typhimurium* and *Escherichia Coli* as Measured by Mutagenicity and by Growth Delay Assays. *Environ. Mutagen.* **1986**, *8*, 659–673.
56. Smirnova, G.; Muzyka, N.; Oktyabrsky, O. Transmembrane Glutathione Cycling in Growing *Escherichia Coli* Cells. *Microbiol. Res.* **2012**, *167*, 166–172.

57. Liu, X.; Sen, S.; Liu, J.; Kulaots, I.; Geohegan, D.; Kane, A.; Puretzky, A. A; Rouleau, C. M.; More, K. L.; Palmore, G. T. R.; et al. Antioxidant Deactivation on Graphenic Nanocarbon Surfaces. *Small* **2011**, *7*, 2775–2785.
58. Riddles, P. W.; Blakeley, R. L.; Zerner, B. Ellman's Reagent: 5,5′-dithiobis(2-Nitrobenzoic Acid)—A Reexamination. *Anal. Biochem.* **1979**, *94*, 75–81.
59. Hou, W.-C.; Chowdhury, I.; Goodwin, D. G.; Henderson, W. M.; Fairbrother, D. H.; Bouchard, D.; Zepp, R. G. Photochemical Transformation of Graphene Oxide in Sunlight. *Environ. Sci. Technol.* **2015**, *49*, 3435–3443.
60. Yang, H.-H.; McCreery, R. L. Elucidation of the Mechanism of Dioxygen Reduction on Metal-Free Carbon Electrodes. *J. Electrochem. Soc.* **2000**, *147*, 3420.
61. Sharma, R.; Baik, J. H.; Perera, C. J.; Strano, M. S. Anomalously Large Reactivity of Single Graphene Layers and Edges toward Electron Transfer Chemistries. *Nano Lett.* **2010**, *10*, 398–405.
62. Qu, D. Investigation of Oxygen Reduction on Activated Carbon Electrodes in Alkaline Solution. *Carbon* **2007**, *45*, 1296–1301.
63. Wang, X.; Quinn, P. J. Vitamin E and Its Function in Membranes. *Prog. Lipid Res.* **1999**, *38*, 309–336.
64. Fuentes, A. M.; Amábile-Cuevas, C. F. Antioxidant Vitamins C and E Affect the Superoxide-Mediated Induction of the soxRS Regulon of *Escherichia Coli*. *Microbiology* **1998**, *144*, 1731–1736.
65. Melegari, S. P.; Perreault, F.; Moukha, S.; Popovic, R.; Creppy, E. E.; Matias, W. G. Induction to Oxidative Stress by Saxitoxin Investigated through Lipid Peroxidation in Neuro 2A Cells and *Chlamydomonas Reinhardtii* Alga. *Chemosphere* **2012**, *89*, 38–43.
66. Hummers, W. S.; Offeman, R. E. Preparation of Graphitic Oxide. *J. Am. Chem. Soc.* **1958**, *80*, 1339.
67. Ellman, G. L. Tissue Sulfhydryl Groups. *Arch. Biochem. Biophys.* **1959**, *82*, 70–77.